Supplementary Text: Modelling structural determinants of ventilation heterogeneity: a perturbative approach.

1 Lung network model

As outlined in the main paper, we have modelled lung regions as symmetrically-branching dyadic (SBD) trees (see Fig 1 in the main text). In reality, the structure is more spatially heterogeneous than this representation, with the number of conducting airway generations varying from $7-20$ [1]. This simplification of the network topology is necessary to apply the perturbative approach developed here.

The airway tree model we have used is lobe-based using the data of Horsfield [1] for the most proximal edges and vertices of the network, denoted by the sets $(\mathcal{E}^{\mathrm{PA}}, \mathcal{V}^{\mathrm{PA}})$. Here the airway geometries are used directly and are listed in S1 Table. More distal branches are represented by seven symmetrically-branching trees labelled $\mathcal{T}_z$ for $z \in \{\mathrm{RU},\ \mathrm{RM},\ \mathrm{RL_{min}},\ \mathrm{RL_{maj}},\ \mathrm{LU},\ \mathrm{LL_{min}},\ \mathrm{LL_{maj}}\}$ representing the lobes, where the lower lobes are split into major and minor sub-trees (see Fig 1 in main text). The calculation of airway and acinus properties from physiological parameters is presented in section 1.4, but first we introduce notation.

1.1 Symmetrically-branching dyadic tree notation

A SB airway tree (see figure SF1) is represented as a one-dimensional network $\mathcal{T}_z = \{\mathcal{V}_z, \mathcal{E}_z\}$ of vertices $\mathcal{V}_z = \left\{\mathcal{V}_z^{\mathrm{cond}}, \mathcal{V}_z^{\mathrm{acin}}\right\}$ such that $\mathcal{V}_z^{\mathrm{cond}} = \left\{v_{z,o}, \left\{v_{z,j,k} \mid 0 \le j < N_z^{\mathrm{cond}},\ 0 \le k < 2^j\right\}\right\}$ is the subset of vertices in the N_z^{cond} generations of conducting airways in the tree where $v_{z,o}$ is the root vertex. The subset $\mathcal{V}^{\mathrm{acin}} = \left\{v_{z,j,k} \mid -1 \le j - N_z^{\mathrm{cond}} < N^{\mathrm{acin}},\ 0 \le k < 2^j\right\}$ is the subset of vertices within the N^{acin} generations of acinar airways (taken to be the same in all lung regions). Subsets of edges are similarly identified such that $\mathcal{E}_z = \left\{\mathcal{E}_z^{\mathrm{cond}}, \mathcal{E}_z^{\mathrm{acin}}\right\}$ where $\mathcal{E}_z^{\mathrm{cond}} = \left\{e_{z,0,0} = \left\{v_{z,o}, v_{z,0,0}\right\}, \left\{e_{z,j,k} = \left\{v_{z,j-1,\lfloor k/2\rfloor}, v_{z,j,k}\right\} \mid v_{z,j,k} \in \mathcal{V}_z^{\mathrm{cond}} \setminus v_{z,o}\right\}\right\}$. The subset of acinar airways is $\mathcal{E}_z^{\mathrm{acin}} = \left\{e_{z,j,k} = \left\{v_{z,j-1,\lfloor k/2\rfloor}, v_{z,j,k}\right\} \mid v_{z,j,k} \in \mathcal{V}_z \setminus \mathcal{V}_z^{\mathrm{cond}}\right\}$. Each vertex in the set of terminal vertices $\Gamma_z \equiv \mathcal{V}_z^{\mathrm{cond}} \cap \mathcal{V}_z^{\mathrm{acin}}$ is connected to the root vertex by a unique (uni-directional) path denoted $\mathcal{P}_{z,o,\alpha} = \left\{e_{z,j,k} \mid j = 0 \ldots N_z^{\mathrm{cond}}, k = \left\lfloor \alpha 2^{j-N_z^{\mathrm{cond}}} \right\rfloor\right\}$. Sub-trees are defined as subsets of vertices and edges in $\mathcal{T}_z$ that form complete trees terminating at the base of $\mathcal{T}_z$ such that $\mathcal{S}_{z,j,k} = \left\{v_{z,j-1,\lfloor k/2\rfloor}, \left\{v_{z,\tilde{j},\tilde{k}}, e_{z,\tilde{j},\tilde{k}} \mid j \le \tilde{j} < N_z^{\mathrm{cond}} + N^{\mathrm{acin}}, k2^j \le \tilde{k} < (k+1)2^j\right\}\right\}$.

To compute the distribution of fluxes on the tree network we consider each acinus as a single three-dimensional volume consisting of numerous alveolar ducts and sacs, that constitute a fraction of the lung parenchyma. The parenchymal volume associated with the tree $\mathcal{T}_z$ is denoted $\Omega_z = \left\{\Omega_{z,\alpha} \subset \mathbb{R}^3 \mid v_{z,N_z^{\mathrm{cond}}-1,\alpha} \in \Gamma_z\right\}$ such that each terminal vertex is connected to a single acinus $\Omega_{z,\alpha}$. We further denote the subset of Ω_z fed by $e_{z,j,k}$ as $\Omega_{z,j,k}$ such that $\Omega_{z,j,k} = \left\{\Omega_{z,\alpha} \mid k2^{N_z^{\mathrm{cond}}-1-j} \le \alpha < (k+1)2^{N_z^{\mathrm{cond}}-1-j}\right\}$. This notation is outlined in figure SF1.

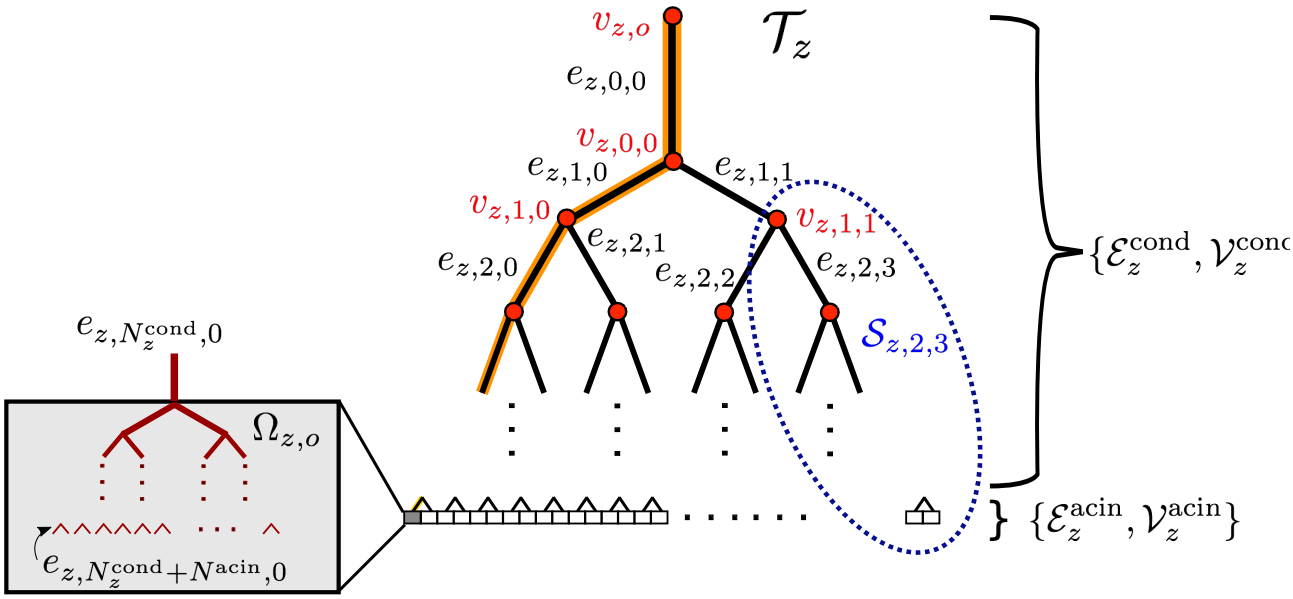

Figure SF1: Sketch of the notation used to identify branches and parenchymal units in the symmetrically branching dyadic tree $\mathcal{T}_z$. Branches $e_{z,j,k}$ (indexed by generation j and branch number k from left to right) form the edges of the network of tubes. The tree terminates in the parenchymal units $\Omega_{z,\alpha}$, and paths (yellow) from the mouth to an acinar unit are labelled $\mathcal{P}_{z,o,\alpha}$. Subtrees (outlined by blue dotted ring) $\mathcal{S}_{z,j,k}$ consist of all vertices that are descendants of vertex $v_{z,j-1,\lfloor k/2 \rfloor}$ and their connecting edges. When calculating gas transport, we consider the acinar branches $\Omega_{z,\alpha}$ from generations $N_z^{\text{cond}} \leq j \leq N_z^{\text{cond}} + N^{\text{acin}}$ (inset).

1.2 Ventilation model

We have assumed Poiseuille flow in each conducting edge of the SB trees $e_{z,j,k} \in \mathcal{E}_z^{\text{cond}}$ and in the proximal airways $e_u \in \mathcal{E}_{\text{PA}}$. The pressure-drop relation is

$$P_{i'} - P_i = \frac{8\pi\mu l_i}{a_i^2} q_i(t), \tag{1}$$

where μ is the air viscosity, q_i is the rate of flux through branch e_i and P_i is the pressure at vertex v_i where we have used i to refer to either a branch in an SB tree $(i) = (z, j, k)$ or in the proximal airways $((i) = (u))$. The vertex $v_{i'}$ is the parent vertex of edge e_i. This underestimates the branch resistance as it does not take into account inertial effects which are significant at all but the most distal branches of the tree. This flow relation can be readily modified to incorporate downstream effects of the bifurcations on the flow profile [2], and such non-linear models remain compatible with the approach outlined here.

At breathing frequency air is approximately incompressible, so conservation of mass dictates

$$q_i(t) = \sum_{\Omega_{z,\alpha} \in \Omega_i} \dot{V}_{z,\alpha}(t), \tag{2}$$

where the volume of gas in $\Omega_{z,\alpha}$ is $V_{z,\alpha}$ and the dot is used to indicate derivatives with respect to time t. If a proximal airway, Ω_u denotes the union of all Ω_z downstream of e_u.

Substituting equation (2) into (1) gives a set of equations describing the flux into each acinus. The pressure-drop relation along the path $\mathcal{P}_{\text{mouth},\alpha} \in \mathcal{L}$ is acquired from summing (1) along each $e_i \in \mathcal{P}_{\text{mouth},\alpha}$ where V_{mouth} denotes the vertex at the proximal end of the tracheal branch. Repeating

this for each $\Omega_{z,\alpha} \in \Omega$ gives a system of $n_{\text{acin}} \equiv \sum_{\mathcal{T}_z \in \mathcal{L}} 2^{N_z^{\text{cond}}}$ coupled Ordinary Differential Equations (ODEs) (*i.e.* one equation for each acinus). In matrix notation these are

$$P_{\text{mouth}}\mathbf{1} - \mathbf{P}(t) = \mathbf{R}_{\text{cond}}\dot{\mathbf{V}}(t), \tag{3}$$

where $\mathbf{P}, \mathbf{V} \in \mathbb{R}^{n_{\text{acin}}}$ have entries $P_{z,\alpha}$ and $V_{z,\alpha}$ corresponding to the pressure and volume for each $\Omega_{z,\alpha} \in \mathcal{L}$. We have assumed that the pressure at vertex $v_{z,N_z^{\text{cond}}-1,\alpha}$ is equal to the gas pressure in the connected acinus $\Omega_{z,\alpha}$. The vector $\mathbf{1}$ is defined as $\mathbf{1} = (1, \ldots, 1)^T \in \mathbb{R}^{n_{\text{acin}}}$ and the elements of the symmetric resistance matrix $\mathbf{R}_{\text{cond}} \in \mathbb{R}^{n_{\text{acin}}} \times \mathbb{R}^{n_{\text{acin}}}$ are

$$\hat{\mathbf{e}}_{\alpha_1}^T \mathbf{R}_{\text{cond}} \hat{\mathbf{e}}_{\alpha_2} = \sum_{e_{j,k} \in \mathcal{P}_{\text{mouth},\alpha_1} \cap \mathcal{P}_{\text{mouth},\alpha_2}} r_i, \tag{4}$$

where the basis vector $\hat{\mathbf{e}}_\alpha = (0, \ldots, 0, 1, 0, \ldots, 0)^T \in \mathbb{R}^{n_{\text{acin}}}$ is non-zero in its α-th element.

To simulate ventilation a constitutive relation is required to determine pressure in the acini Ω. Each acinus is comprised of a network of alveolar ducts and sacs embedded within the fibrous lung parenchyma. We represent the dynamics of this complex medium with a simple visco-elastic volume, such that each acinus has linear elasticity $K_{z,\alpha}$ and resistance $R_{z,\alpha}$ such that

$$P_{z,\alpha} = \left(P_{\text{mouth}} + P_{z,\alpha}^{(\text{pl})}(t) - P_{z,\alpha}^{(\text{pl0})}\right) + K_{z,\alpha}(V_{z,\alpha}(t) - V_{z,\alpha}^*) + R_{z,\alpha}\dot{V}_{z,\alpha}(t), \tag{5}$$

where $V_{z,\alpha}^*$ is the resting volume of $\Omega_{z,\alpha}$, $P_{z,\alpha}^{(\text{pl})}$ is the intrapleural pressure acting on $\delta\Omega_{z,\alpha}$, and $P_{z,\alpha}^{(\text{pl0})}$ is the reference stationary value of the intrapleural pressure (when $V_{z,\alpha} = V_{z,\alpha}^*$ and $\dot{V}_{z,\alpha} = 0$). In general, the local intrapleural pressure $P_{z,\alpha}^{(\text{pl0})}$ can depend on the volumes and inflation rates of the surrounding acini. We have considered only the simplest case here $P_{z,\alpha}^{(\text{pl})}(t) = P_{\text{pl}}(t)$ and $P_{z,\alpha}^{(\text{pl0})} = P_{\text{pl0}}$ for all $\Omega_{z,\alpha} \in \mathcal{L}$, such that the pressure applied to all acini have identical properties.

Substituting equation (5) into equation (3) gives the following set of linear equations for the full ventilation dynamics,

$$\left(\mathbf{R}_{\text{cond}} + \mathbf{R}_{\text{acin}}\right)\dot{\mathbf{V}}(t) + \mathbf{K}\left(\mathbf{V}(t) - \mathbf{V}^*\right) = \left(P_{\text{pl0}} - P_{\text{pl}}(t)\right)\mathbf{1}, \tag{6}$$

where $\mathbf{V}^* \in \mathbb{R}^{n_{\text{acin}}}$ is the vector of resting volumes $V_{z,\alpha}^*$ of the parenchymal sub-units and the matrix $\mathbf{K} \in \mathbb{R}^{n_{\text{acin}}} \times \mathbb{R}^{n_{\text{acin}}}$ is diagonal with entries $K_{z,\alpha}$, and similarly $\mathbf{R}_{\text{acin}} \in \mathbb{R}^{n_{\text{acin}}} \times \mathbb{R}^{n_{\text{acin}}}$ is diagonal with entries $R_{z,\alpha}$. In a more complex description with linear mechanical coupling between acini, the matrices $\mathbf{R}_{\text{acin}}$ and $\mathbf{K}$ could have off-diagonal entries. The linear ventilation equations used here have a direct electrical analogue where the acinus is modelled a capacitor and resistor in series, while airways are a network of resistors with current q and potential P at the vertices.

1.3 Transport model

Gas transport on the network is modelled as one-dimensional advection-diffusion in each airway, with transport into the alveolar sacs accounted for by-a two cylinder model adopted in [3, 4]. The volume fraction of inert tracer gas on edge $e_i \in \mathcal{L}$ (we use i generically to refer to any index or indices that refer to a branch in the network) is modelled as a one-dimensional (cross-sectionally averaged) concentration field $c_i(x,t)$ where x is the distance along the edge from its parent vertex $v_{i'}$. Thus, in this convention, inspiratory (expiratory) flows are those directed down (up) the tree and are positive

(negative).

The ventilation model in the previous section treats the parenchyma as a three-dimensional visco-elastic domain connected to the end of the tree. However, the detailed internal structure of the acinus is important to modelling gas transport. Therefore, we use the idealised gas-transport equations outlined in [5] which represents each acinus $\Omega_{z,\alpha}$ by the sub-tree $\mathcal{S}_{z,N^{\text{cond}},\alpha} \equiv \mathcal{S}^{\text{acin}}_{z,\alpha}$ such that $\bigcup_{\alpha\in\mathcal{T}_z} \mathcal{S}^{\text{acin}}_{z,\alpha} = \left\{\mathcal{E}^{\text{acin}}_z, \mathcal{V}^{\text{acin}}_z\right\}$.

In each acinus $\Omega_{z,\alpha}$ the tubes are lined with alveoli, which is accounted for by writing the total tube cross-section as $A_i(t) = a_i + n_i^{(\text{sac})} V^{(\text{sac})}(t)/l_i \ \forall e_i \in \mathcal{E}^{\text{acin}}_{z,\alpha}$ where a_i is the cross-section of the alveolar duct (assumed rigid) and the second term is the alveolar sac volume per unit length on the branch $e_{z,j,k}$. In particular n_i^{sac} is the number of alveolar sacs lining e_i and $V^{\text{sac}}(t)$ is the volume of each alveolar sac in the acinus. Following [5], we have assumed that all alveolar sacs in a given acinus are identical and inflate at the same rate. Average anatomical data [6] suggest that the number of alveoli lining a branch in the acinus is proportional to the duct surface area $l_i\sqrt{a_i}$ with a correction factor $0 < \Phi_i \leq 1$ which depends only on the branch generation relative to the terminal bronchiole generation $j - N_z^{\text{cond}}$ (a detailed parameter list is given in S1 Table). Therefore the total branch cross-section in each acinus can be written

$$A_i(t) = a_i + V_{z,\alpha}(t)\Phi_i\sqrt{a_i} \Bigg/ \left(\sum_{e_{\tilde{i}}\in\mathcal{S}^{\text{acin}}_{z,\alpha}} \Phi_{\tilde{i}} l_{\tilde{i}} \sqrt{a_{\tilde{i}}} \right) \quad \forall e_i \in \mathcal{S}^{\text{acin}}_{z,\alpha} \ , \forall \mathcal{S}^{\text{acin}}_{z,\alpha} \in \mathcal{L}. \tag{7}$$

Note that we consistently define $A_i = a_i$ for all branches in the conducting network $e_i \in \mathcal{E}^{\text{cond}}$ (where $\mathcal{E}^{\text{cond}} = \mathcal{E}_{UA} \cup (\bigcup_{\mathcal{T}_z\in\mathcal{L}} \mathcal{E}^{\text{cond}}_z)$), where there are no alveolar sacs.

We approximate the gas concentration as well-mixed in the radial direction, but unable flow directly between sacs in the acinus. Within a conducting branch the flux is taken to be

$$F_i(x,t) = a_i \left[u_i(t)c_i(x,t) - D_i(t)\frac{\partial c_i(x,t)}{\partial x} \right] \quad \forall e_i \in \mathcal{E}^{\text{cond}}, \tag{8}$$

where $u_i = q_i/a_i$ is the flow velocity in the tube and the diffusion coefficient $D_i(x,t) = D_0 + Cu_i(x,t)a_i$ is corrected for Taylor-like dispersion in a branching tube network, where $C = 1.08$ for inspiration and $C = 0.37$ for expiration [7]. In the acinar branches, we assume no flow-dependent dispersion rate as we know of no such relations derived for this complex expanding geometry and the flux relation is

$$F_i(x,t) = a_i u_i(x,t)c_i(x,t) - D_0 \left[\phi A_i(t) + (1-\phi)a_i\right] \frac{\partial c_i(x,t)}{\partial x} \quad \forall e_i \in \mathcal{E}^{\text{acin}}_z \, , \forall \mathcal{E}^{\text{acin}}_z \in \mathcal{L}, \tag{9}$$

where ϕ is a phenomenological parameter that sets the fraction of alveolar sac cross-section that is involved in diffusion [4] (see S1 Table).

Mass conservation and incompressibility conditions for branch $e_{j,k}$ are given by

$$\frac{\partial}{\partial t}\left[A_i(t)c_i(x,t)\right] = -\frac{\partial F_i(x,t)}{\partial x} - G_i(x,t,c_{j,k}) \quad \forall e_i \in \mathcal{L}, \tag{10}$$

$$\frac{1}{a_i}\frac{\partial A_i(t)}{\partial t} + \frac{\partial u_i(x,t)}{\partial x} = 0 \quad \forall e_i \in \mathcal{L}. \tag{11}$$

We have included here a generic uptake/source term G_i to account for gas exchange in the alveoli, but for the purposes of inert gas washout tests we assume that uptake is negligible and $G_i = 0$ throughout. Equation (11) defines the air velocity everywhere, given that it is zero at all endpoints

$V_{N_z^{\text{cond}}+N_z^{\text{acin}}-1,k} \in \mathcal{T}_z$ for all $\mathcal{T}_z \in \mathcal{L}$ and A_i is calculated consistently by equation (7). This, in turn, is calculated from the acinar volumes computed in equation (6). Flux conservation implies continuity of the concentration field at branching points, but a discontinuity in the gradient.

1.4 Mean-path model of the lung

The model can be made more computationally efficient by replacing sub-trees with mean-path models. In this way, simulations can incorporate the effects of heterogeneity to a certain depth, then average the remainder of the structure. A mean-path model approximates a sub-tree by taking every airway in a given generation to have identical geometry, represented by the mean airway geometry for that tree.

Replacing a particular sub-tree $\mathcal{S}_{z,j',k'}$ with a mean-path model changes how we represent this in the network $\mathcal{T}_z$ (figure SF2). As all branches in the sub-tree are assumed to behave in an identical manner, they can be simply represented by a single edge or series of edges. The network becomes $\bar{\mathcal{T}}_z = (\mathcal{T}_z \setminus \mathcal{S}_{z,j',k'}) \cup \bar{\mathcal{S}}_{z,j',k'}$ (see figure SF2) where

$$\bar{\mathcal{S}}_{z,j',k'} = v_{z,j'-1,\lfloor k'/2 \rfloor} \cup \left\{ \left\{ \bar{e}_{z,j}^{(j',k')}, \bar{v}_{z,j}^{(j',k')} \right\} \mid j' \leq j < N_z^{\text{cond}} + N^{\text{acin}} \right\}. \tag{12}$$

Each mean-path edge $\bar{e}_{z,j}^{(j',k')}$ and vertex $\bar{v}_{z,j}^{(j',k')}$ (signified by the over-bar) represents all the branches in generation j of the original sub-tree $\mathcal{S}_{z,j',k'}$. The total duct cross-section associated with $\bar{e}_{z,j}^{(j',k')}$ is $\bar{s}_{z,j}^{(j',k')} = 2^{j-j'} \bar{a}_{z,j}^{(j',k')}$ where $\bar{a}_{z,j}^{(j',k')}$ is the mean branch cross-section of generation j in $\mathcal{S}_{z,j',k'}$. The

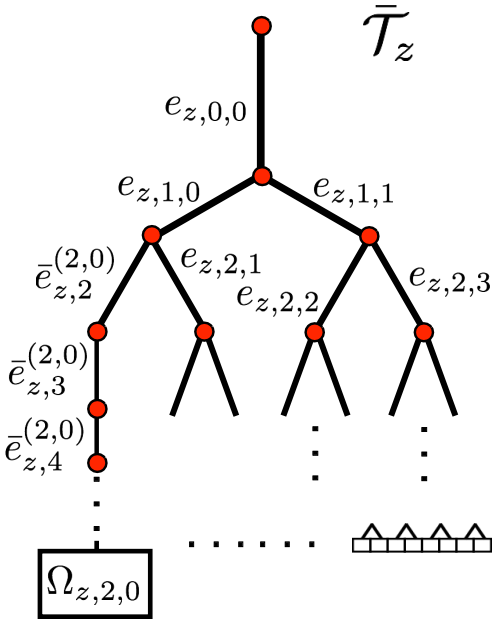

Figure SF2: A mean-path tree network $\bar{\mathcal{T}}_z$ with sub-tree $\mathcal{S}_{z,2,0}$ replaced by a mean-path.

effective resistance of edge $\bar{e}_{z,j}^{(j',k')}$ is that of $2^{j-j'}$ Poiseuille resistors in parallel such that

$$\bar{r}_{z,j}^{(j',k')} = \frac{8\pi\mu \bar{l}_{z,j}^{(j',k')}}{2^{j-j'}(\bar{a}_{z,j}^{(j',k')})^2}. \tag{13}$$

this effective resistance is computed from the mean geometry, which is different to the mean resistance

of branches with different geometries. The pressure-flow relation over the edges $\bar{e}_{z,j}^{(j',k')} \in \bar{\mathcal{E}}^{\text{cond}}$ is

$$\left(\bar{R}^{\text{acin}}_{z,j',k'} + \sum_{j=j'}^{N_z^{\text{cond}}} \bar{r}_{z,j}^{(j',k')}\right) \dot{V}_{z,j',k'} + K_{z,j',k'}\left(V_{z,j',k'} - V^{\star}_{z,j',k'}\right) = P_{z,j'-1,\lfloor k'/2 \rfloor} - \bar{P}^{(j',k')}_{N_z^{\text{cond}}}, \tag{14}$$

where the bulk acinus properties are

$$\begin{aligned} K_{z,j',k'} &= 4^{j'-N_z^{\text{cond}}} \sum_{\alpha \in \Omega_{z,j',k'}} K_{z,\alpha}\,, \quad R^{\text{acin}}_{z,j',k'} = 4^{j'-N_z^{\text{cond}}} \sum_{\alpha \in \Omega_{z,j',k'}} R_{z,\alpha}, \\ V^{\star}_{z,j',k'} &= \sum_{\alpha \in \Omega_{z,j',k'}} V^{\star}_{z,\alpha}. \end{aligned} \tag{15}$$

Thus, the mean-path model represents the whole sub-tree $\mathcal{S}_{z,j',k'}$ with a single path terminating in a collection of identical acini with collective elastance $K_{z,j',k'}$ and total alveolar volume $V_{z,j',k'}$. The resistances remain unchanged for all $e_{z,j,k} \in \bar{\mathcal{T}} \backslash \bar{\mathcal{S}}_{z,j',k'}$, *i.e.* those edges not included in the mean-path.

The mean-path pressure-drop equation then replaces the subtree $\mathcal{S}_{z,j',k'}$ in the set of ventilation ODEs, which is solved as before (see section 1.2). Conservation of mass and incompressibility on sub-tree $\bar{\mathcal{S}}_{z,j',k'}$ give the following mean-path transport equation

$$\frac{\partial}{\partial t}\left[S_{z,j}(t)\bar{c}_{z,j}(\bar{x},t)\right] + \frac{\partial}{\partial \bar{x}}\left[s_{z,j}\bar{u}_{z,j}(\bar{x},t)\bar{c}_{z,j}(\bar{x},t)\right] = \frac{\partial}{\partial \bar{x}}\left[\bar{D}_{z,j}s_{z,j}(\bar{x},t)\frac{\partial \bar{c}_{z,j}(\bar{x},t)}{\partial \bar{x}}\right], \tag{16}$$

$$\frac{1}{s_{z,j}}\frac{\partial S_{z,j}(t)}{\partial t} + \frac{\partial \bar{u}_{z,j}(x,t)}{\partial x} = 0. \tag{17}$$

where we have omitted the superscripts (j',k') on all airway properties for clarity. The total cross-section of all the mean-path ducts plus alveoli is $S_{z,j} = 2^{j-j'}\bar{A}_{z,j}$. The distance coordinate $\bar{x} = \sum_{\tilde{j}=j'}^{j-1} \bar{l}_{z,\tilde{j}} + \bar{l}_{z,j}\,(x/l_{z,j,k})$, for any $\left\{l_{z,j,k} \mid e_{z,j,k} \in \mathcal{S}_{z,j',k'}\right\}$ is scaled by the mean branch length. The mean path velocity $\bar{u}_{z,j}(x,t)$ and the effective diffusion coefficient $\bar{D}_{z,j}(x,t)$ are computed from the mean airway geometry. There is again a discontinuity in cross-section at the generation boundaries, which in turn implies a discontinuity in concentration gradient so that diffusive flux is conserved, and a discontinuity in flow rate so that concentration is assumed consistent. This is dealt with numerically using the finite volume method outlined in section 2.

In the simplest case, one can represent the whole network $\mathcal{T}_z$ with a mean-path model (often referred to as a "trumpet model"). Here, we use this mean-path representation ($\mathcal{T}_z \to \bar{\mathcal{S}}_{z,0,0}$) to describe each lung region ($z \in \{\text{RU, RM, RL}_{\text{min}}, \text{RL}_{\text{maj}}, \text{LU, LL}_{\text{min}}, \text{LL}_{\text{maj}}\}$) in the baseline case, before modelling the effect of weak heterogeneity. The baseline properties of the airways in the different lung regions are set to be equal for each Strahler order. We have chosen $N^{\text{cond}}_{RU} = N^{\text{cond}}_{LU} = N^{\text{cond}}_{RL_{\text{maj}}} = N^{\text{cond}}_{LL_{\text{maj}}} = 13$, $N^{\text{cond}}_{RM} = 12$ and $N^{\text{cond}}_{RL_{\text{min}}} = N^{\text{cond}}_{LL_{\text{min}}} = 11$. Conducting airway diameter and length have a fixed ratio LD_{cond} and each airway scales with its parent branch according to the Murray–Hess law

$$\bar{a}_{z,j} = \pi\left(\frac{\bar{l}_{z,j}}{2LD_{\text{cond}}}\right)^2, \tag{18}$$

$$\bar{l}_{z,j+1} = \lambda \bar{l}_{z,j} \quad \forall \bar{e}_{z,j} \in \bar{\mathcal{E}}^{\text{cond}}_z \quad \forall \mathcal{T}_z \in \mathcal{L} \tag{19}$$

where $\lambda \approx 2^{-1/3}$. The volume of the conducting airways is fitted to their total volume $V_D - V_{\text{PA}}$ where V_D is the anatomical dead-space (excluding the mouth) and V_{PA} is the volume of the airways in $\mathcal{E}^{\text{PA}}$,

such that

$$\bar{l}_{RU,0} = \left(\frac{4LD_{\text{cond}}^2 \left(V_D - V_{\text{PA}}\right)}{\pi \sum_{\mathcal{T}_z \in \mathcal{L}} \sum_{j=0}^{N_z^{\text{cond}}-1} \lambda^{3(12-j)}} \right)^{1/3}, \tag{20}$$

and $\bar{l}_{z,0} = \lambda^{13-N_z^{\text{cond}}} \bar{l}_{RU,0}$. All acini have been treated as identical in the baseline model with constant length and area scaling between parent and daughter ducts of λ_{acin} and a fixed ratio of length to diameter LD_{acin},

$$\bar{a}_{z,j} = \pi \left(\frac{\bar{l}_{z,j}}{2LD_{\text{acin}}} \right)^2, \tag{21}$$

$$\bar{l}_{z,j+1} = \lambda_{\text{acin}} \bar{l}_{z,j} \quad \forall \bar{e}_{z,j} \in \bar{\mathcal{E}}_z^{\text{acin}} \quad \forall \mathcal{T}_z \in \mathcal{L}. \tag{22}$$

The acinar ducts constitute a fraction $V_{\text{duct}}/V_{\text{acin}}$ of the total acinar volume and so fitting the volume to the physiological parameters gives

$$\bar{l}_{z,N_z^{\text{cond}}} = \left(\frac{4LD_{\text{acin}}^2 V_{\text{duct}} \left(V_{\text{FRC}} - V_{\text{D}}\right)}{\pi V_{\text{acin}} \sum_{\mathcal{T}_z \in \mathcal{L}} \sum_{j=N_z^{\text{cond}}}^{N_z^{\text{acin}}} \lambda^{3j}} \right)^{1/3} \forall \mathcal{T}_z \in \mathcal{L}. \tag{23}$$

This representation in results in $2^{15} + 2^{13}$ terminal bronchioles, which is an overestimate of Weibel's estimate (30,000) [8], but accounts well for the relative lobe volumes [1].

1.5 Limit of weak heterogeneity

The geometry of the airways and acinar elastance can be described in terms of deviations from the mean-path model of the whole network (where $\mathcal{T}_z \to \bar{\mathcal{S}}_{z,0,0}$). The superscript $(0,0)$ is implied for all mean-path edge properties, and hence is omitted throughout this section for clarity (*e.g.* $\bar{a}_{z,j}^{(0,0)} \equiv \bar{a}_{z,j}$). We write $a_{z,j,k} = \bar{a}_{z,j}(1 + \epsilon_{z,j,k}^{(a)})$, $l_{z,j,k} = \bar{l}_{z,j}(1 + \epsilon_{z,j,k}^{(l)})$ and $K_{z,\alpha} = 2^{-N_z^{\text{cond}}} K_{z,0,0}(1 + \epsilon_{z,j,k}^{(K)})$ such that the ϵ parameters measure the individual airway deviation from the mean-path value. In the limit of small perturbations the resistance can be approximated as linear with respect to the ϵ parameters

$$r_{z,j,k} \approx \bar{r}_{z,j} \left(1 + \epsilon_{z,j,k}^{(l)} - 2\epsilon_{z,j,k}^{(a)}\right). \tag{24}$$

In this limit of $\epsilon \ll 1$, the change in any output variable $g \in \{A, c, u, D\}$ in the tree $\mathcal{T}_z$ can be expressed as a linear superposition of the contributions from each perturbation

$$\Delta g_{z,j,k} \equiv g_{z,j,k} - \bar{g}_{z,j} = \sum_{p} \sum_{\mathcal{T}_{z'} \in \mathcal{L}} \sum_{e_{j',k'} \in \mathcal{T}_{z'}} \delta g_{z,j,k}^{(p,z',j',k')} \epsilon_{z',j',k'}^{(p)} + O(\epsilon^2). \tag{25}$$

The linear sensitivity functions $\delta g_{z,j,k}^{(p,z',j',k')}$ are degenerate with respect to branch numbers k and k' due to symmetry at zeroth order. First, if the measured variable is in a different mean-path to the perturbation ($z' \neq z$, including the proximal airways) then the response is independent of branch number (as all branches in a given generation of a mean path are identical at zeroth order). Secondly, if the measured variable is in the same mean-path as the perturbation ($z' = z$), then the linear sensitivity is dependent only on the generation of the lowest common ancestor (LCA) of $e_{z,j,k}$ and

$e_{z,j',k'}$ and their respective generations. These can be summarised by

$$\delta g_{z,j,k}^{(p,z',j',k')} = \delta_{z,z'}\delta g_{z,j}^{(p,j',j_{\mathrm{LCA}})} + (1-\delta_{z,z'})\delta g_{z,j}^{(p,z',j')} \tag{26}$$

where

$$\delta g_{z,j}^{(p,j',j_{\mathrm{LCA}})} \equiv \delta g_{z,j,k}^{(p,z,j',k')} \quad \forall\, \{e_{z,j,k}, e_{z,j',k'}\} \in \mathcal{T}^z \tag{27}$$

$$\delta g_{z,j}^{(p,z',j')} \equiv \delta g_{z,j,k}^{(p,z',j',k')} \quad \forall\, e_{z,j,k} \in \mathcal{T}^z,\ e_{z,j',k'} \in \mathcal{T}^{z'} \neq \mathcal{T}^z. \tag{28}$$

The parameter $j_{\mathrm{LCA}} \equiv j_{\mathrm{LCA}}(z,j,k,j',k')$ is the generation number of the LCA of branches $e_{z,j,k}$ and $e_{z,j',k'}$,

$$j_{\mathrm{LCA}}(z,j,k,j',k') = \max\left\{\tilde{j} \mid e_{z,\tilde{j},\tilde{k}} \in \mathcal{P}_{z,o,k2^{N_z^{\mathrm{cond}}-j}} \cap \mathcal{P}_{z,o,k'2^{N_z^{\mathrm{cond}}-j'}}\right\}. \tag{29}$$

Thus, linear sensitivities need only be calculated for one perturbation to each generation of the SBD networks $\mathcal{T}_{z'}$. Without loss of generality, we choose to always perturb the left-most branch in each case, *i.e.* $k'=0$. The response to the perturbation of $e_{z',j',0}$ on $\mathcal{L}$ is calculated by replacing the sub-trees $\mathcal{S}_{z',j,k} \in \mathcal{S}_{z',j',0} \cup \left\{\mathcal{S}_{\tilde{j},1} \mid 0 < \tilde{j} \leq j'\right\}$ with mean-paths, as shown in figure SF3. We use $\bar{\mathcal{T}}_{z',j'}$ to denote this particular tree, and $\mathcal{L}_{z',j'}$ to denote the resulting whole lung network, that is used to simulate the response to a single perturbation at $e_{j',0}$.

The linear perturbation to the ventilation equation (6) on $\mathcal{L}_{z',j'}$ is

$$\begin{aligned}&\left(\bar{\mathbf{R}}_{z',j'}^{(\mathrm{cond})} + \bar{\mathbf{R}}_{z',j'}^{(\mathrm{acin})}\right)\Delta\dot{\mathbf{V}} + \bar{\mathbf{K}}_{z',j'}\Delta\mathbf{V} \\ &+ \left(\Delta r_{z',j',0}\dot{V}_{z',j',0} + \Delta K_0 V_{z',j',0}\delta_{j',N_z^{\mathrm{cond}}}\right)\hat{\mathbf{e}}_{z',j',0} = -\Delta P^{(\mathrm{pl})}(t)\mathbf{1},\end{aligned} \tag{30}$$

where the resistance and stiffness matrices $\bar{\mathbf{R}}_{z',j'}, \bar{\mathbf{K}}_{z',j'} \in \mathbb{R}^{7+j'} \times \mathbb{R}^{7+j'}$ consist of the mean-path parameters of order $O(\epsilon^0)$ on the network $\mathcal{L}_{z',j'}$, and $\Delta\mathbf{V} = (\Delta V_{z_1\neq z',0,0}, \ldots, \Delta V_{z_6\neq z',0,0}, \Delta V_{z',1,1}, \ldots, \Delta V_{z',j',0}, \Delta V_{z,'j',1})$ is the vector of $O(\epsilon^1)$ changes to the acinar volumes in $\mathcal{L}_{z',j'}$. The first six entries are the volume changes in the unperturbed SBD trees ($\mathcal{T}_z$ for $z \neq z'$), and the remainder are sub-trees of the perturbed tree $\bar{\mathcal{T}}'_{z',j'}$. The perturbation contributes only to a single entry in either one of these tensors, namely the diagonal entry associated with perturbed sub-tree $\bar{\mathcal{S}}_{z',j',0}$ shown by the basis vector $\mathbf{e}_{z',j',0}$ such that $\Delta\mathbf{V}^T\hat{\mathbf{e}}_{z',j',k'} = \Delta V^{z',j',0}$. Equation (30) is solved for $\Delta\mathbf{V}$ at each time step by inverting the equation under the constraint that the flow rate at the mouth is prescribed $\mathbf{1}^T\Delta\dot{\mathbf{V}} = 0$, which sets the pressure perturbation $\Delta P^{(\mathrm{pl})}(t)$.

The solution of equation (30) gives the perturbed volumes of the parenchymal units, which are then distributed on to the tree using equation (7) to linear order in the perturbations

$$\begin{aligned}\Delta A_i = \Delta a_i + \Bigg\{&\Delta V_{z,\alpha}(t)\Phi_i\sqrt{\bar{a}_i} + V_{z,\alpha}(t)\Phi_i\frac{\Delta a_i}{2\sqrt{\bar{a}_i}} \\ &- \left[\sum_{e_{\tilde{i}}\in\mathcal{S}_{z,\alpha}^{\mathrm{acin}}} \Phi_{\tilde{i}}\left(\Delta l_{\tilde{i}}\sqrt{\bar{a}_{\tilde{i}}} + \bar{l}_{\tilde{i}}\frac{\Delta a_{\tilde{i}}}{2\sqrt{\bar{a}_{\tilde{i}}}}\right)\right] \Bigg/ \left[\sum_{e_{\tilde{i}}\in\mathcal{S}_{z,\alpha}^{\mathrm{acin}}} \Phi_{\tilde{i}}\bar{l}_{\tilde{i}}\sqrt{\bar{a}_{\tilde{i}}}\right]\Bigg\} \Bigg/ \left(\sum_{e_{\tilde{i}}\in\mathcal{S}_{z,\alpha}^{\mathrm{acin}}} \Phi_{\tilde{i}}\bar{l}_{\tilde{i}}\sqrt{\bar{a}_{\tilde{i}}}\right)\end{aligned} \tag{31}$$

$$\forall e_i \in \mathcal{S}_{z,\alpha}^{\mathrm{acin}}\ ,\ \forall \mathcal{S}_{z,\alpha}^{\mathrm{acin}} \in \mathcal{L}_{z',j'}.$$

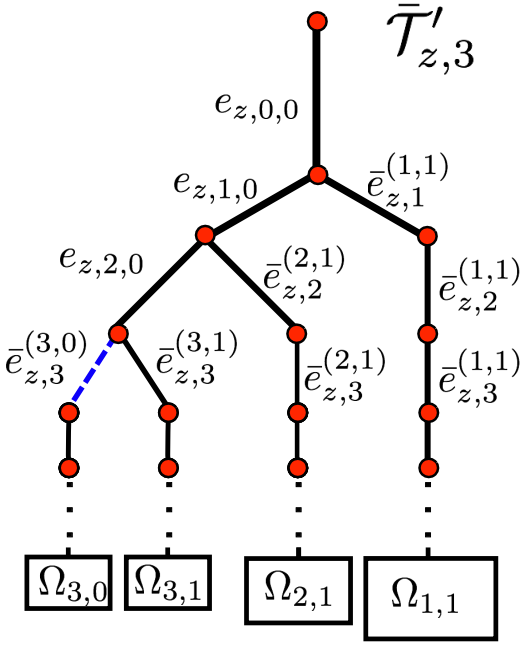

Figure SF3: Perturbed network $\bar{\mathcal{T}}'_{z'}$ for a perturbation of branch $e_{3,0}$ (dashed blue line) resulting in four terminal sub-trees which account for $1/8, 1/8, 1/4, 1/2$ of the total acinar volume respectively from left to right in the diagram.

Finally, the $O(\epsilon^1)$ concentration field is computed by the linearised form of (10) as

$$\begin{aligned}
&\frac{\partial}{\partial t}\left[\bar{c}_i\bar{S}_i\left(\frac{\Delta c_i}{\bar{c}}+\frac{\Delta A_i}{\bar{A}_i}\right)\right]+\frac{\partial}{\partial \bar{x}}\left[\bar{u}_i\bar{s}_i\bar{c}_i\left(\frac{\Delta u_i}{\bar{u}_i}+\frac{\Delta a_i}{\bar{a}_i}+\frac{\Delta c_i}{\bar{c}_i}\right)\right]\\
&\quad=\frac{\partial}{\partial \bar{x}}\left[\bar{D}_i\bar{s}_i\frac{\partial \bar{c}_i}{\partial \bar{x}}\left(\frac{\Delta D_i}{\bar{D}_i}+\frac{\Delta s_i}{\bar{s}_i}+\frac{\partial \Delta c_i/\partial \bar{x}}{\partial \bar{c}_i/\partial \bar{x}}-\frac{\Delta l_i}{\bar{l}_i}\frac{\partial \bar{c}_i}{\partial \bar{x}}\right)\right] \qquad (32)\\
&\qquad+\frac{\Delta l_i}{\bar{l}_i}\frac{\partial}{\partial \bar{x}}\left(\bar{u}_i\bar{s}_i\bar{c}_i\right)-\frac{\Delta l_i}{\bar{l}_i}\frac{\partial}{\partial \bar{x}}\left(\bar{D}_i\bar{s}_i\frac{\partial \bar{c}_i}{\partial \bar{x}}\right),\\
&\frac{\partial \Delta S_i}{\partial t}+\frac{\partial}{\partial x}\left[\bar{s}_i\bar{u}_i\left(\frac{\Delta u_i}{\bar{u}_i}+\frac{\Delta s_i}{\bar{s}_i}\right)\right]=0. \qquad (33)
\end{aligned}$$

The quantities Δs_i and ΔS_i are the absolute changes in total cross-sectional area in branch j of tree i, hence the factor of 2^{j_s}. The branch length change Δl_i is non-zero only in the perturbed branch $j = j_p$ and $i = 2j_p + 1$, and so the distance along the tree is still given in terms of the x-coordinate on the symmetric tree $\bar{x}$.

2 Numerical simulation of coupled ventilation and transport

We have numerically integrated the ventilation equation (6) using the Crank–Nicholson scheme

$$\left(\mathbf{R}+\delta t\frac{\mathbf{K}}{2}\right)\mathbf{V}^{n+1}=\left(\mathbf{R}-\delta t\frac{\mathbf{K}}{2}\right)\mathbf{V}^{n}+\delta t\left[\mathbf{K}\mathbf{V}^{*}+\left(P_{\mathrm{pl0}}-\frac{1}{2}\left(P^{n}_{\mathrm{pl}}+P^{n+1}_{\mathrm{pl}}\right)\right)\mathbf{1}\right], \qquad (34)$$

where δt is the discretised time-step ($\delta t = 0.025$s used for all simulations) and the superscripts of the dynamic quantities indicate time-step, *e.g.* $\mathbf{V}^n = \mathbf{V}(t = n\delta t)$. Given a prescribed function for P_{pl}, this equation can be solved by direct inversion. We choose to prescribe the net flow instead, and infer the pleural pressure at each time-step due to this constraint. The linear system of equations then

becomes

$$\begin{pmatrix} \mathbf{A} & \mathbf{1} \\ \mathbf{1}^T & 0 \end{pmatrix} \begin{pmatrix} \mathbf{V}^{n+1} \\ \delta t P_{\mathrm{pl}}^{n+1}/2 \end{pmatrix} = \begin{pmatrix} \mathbf{B} & -\mathbf{1} \\ \mathbf{1}^T & 0 \end{pmatrix} \begin{pmatrix} \mathbf{V}^{n} \\ \delta t P_{\mathrm{pl}}^{n}/2 \end{pmatrix} + \delta t \begin{pmatrix} \mathbf{K}\mathbf{V}^* + P_{\mathrm{pl0}}\mathbf{1} \\ \dot{q}_{\mathrm{mouth}}\left((n+1/2)\delta t\right) \end{pmatrix} \tag{35}$$

where $\mathbf{A} = \mathbf{R} + \delta t\mathbf{K}/2$ and $\mathbf{B} = \mathbf{R} - \delta t\mathbf{K}/2$. The bottom line of (35) ensures that the total flow rate at time $t = (n+1/2)\delta t$ is set by the prescribed function $\dot{q}_{\mathrm{mouth}}(t)$. This system is solved in C++ using the Eigen [9] factorisation routine 'PartialPivLU'. We initialise the simulation with $\mathbf{V}^0 = \mathbf{V}^*$ and run the ventilation solver for 25 breaths before initiating the simulation of washout to reach a stationary breathing pattern.

At each time step the cross-section of the acinar airways are calculated through equation (7). Note that in general the tree structure may contain mean path branches, which in turn my contain a whole acinus, or part of single acinus (depending on the tree structure being simulated). To simulate gas transport we discretise the network of edges $e_i \in \mathcal{L}$ into finite volume elements $w_{i,x}$ for $x \in \{0, 1, \ldots, p_i - 1\}$ (see Fig SF4) where p_i is the number of volumes that constitute the branch e_i. We define each volume in a branch to have equal length

$$h_{i,x} = l_i/p_i \quad \forall w_{i,x} \in e_i, \tag{36}$$

and choose p_i as the maximum of either $p_{\min}$, the quantity $\lfloor Pe(l_i)/Pe_{\min} \rfloor$, or $\lfloor l_i/(0.025L) \rfloor$ where $Pe(l_i)$ estimates the maximum longitudinal Peclet number of the branch i and $Pe_{\min}$ is the minimum volume element Peclet number. The distance L is the length of any path from the mouth the end point of $\mathcal{T}^{(\mathrm{RL_{maj}})}$. We have chosen $p_{min} = 1$ and $Pe_{\min} = 10$ for conducting branches and $p_{\min} = 4$ and $Pe_{\min} = \infty$ for acinar ducts. Thus each branch in the conducting zone consists of at least one finite volume, and each acinar duct at least four. These values were chosen following tests varying these parameters independently and recording the convergence to a solution (see documentation accompanying code at [10]). We write the cross-sections of branch e_i in terms of s_i and S_i to account for the possibility that e_i is in a mean-path. Each volume unit $w_{i,x} \in e_i$ also has equal cross-section, and therefore equal volume. Each volume unit $w_{i.x} \in e_i$ has concentration $c_{i,x}$, and velocity $u_{i,x}^{(l)}, u_{i,x}^{(r)}$ and diffusion coefficients $D_{i,x}^{(l)}, D_{i,x}^{(r)}$ defined at the left and right edges. The velocities at time $(n+1/2)\delta t$ are calculated through the incompressibility equation as

$$u_{i,x}^{(l)} = u_{i,x}^{(r)} + \frac{h_{i,x}}{\delta t}\left(S_{i,x}^{n+1} - S_{i,x}^{n}\right), \tag{37}$$

$$u_{i,x}^{(r)} = \left(\frac{s_{i,x+1}}{s_{i,x}}\right) u_{i,x+1}^{(l)}. \tag{38}$$

At a terminating branch ($e_i = e_{z,N_z^{\mathrm{cond}}+N^{\mathrm{acin}},k} \in \mathcal{L}$) the final volume-unit has velocity boundary condition $u_{i,p_i-1}^{(r)} = 0$. At a bifurcation, conservation of flux means

$$u_{i,p_i-1}^{(r)} = \frac{1}{s_{i,p_i-1}}\left(u_{i_{d1},0}^{(l)} s_{i_{d1},0} + u_{i_{d2},0}^{(l)} s_{i_{d2},0}\right) \tag{39}$$

where $e_{i_{d1}}$ and $e_{i_{d2}(i)}$ are the daughter branches of e_i. The no-flow boundary conditions equations (37), (38), and (39) fully define the velocity everywhere on the tree. The final step is to update the

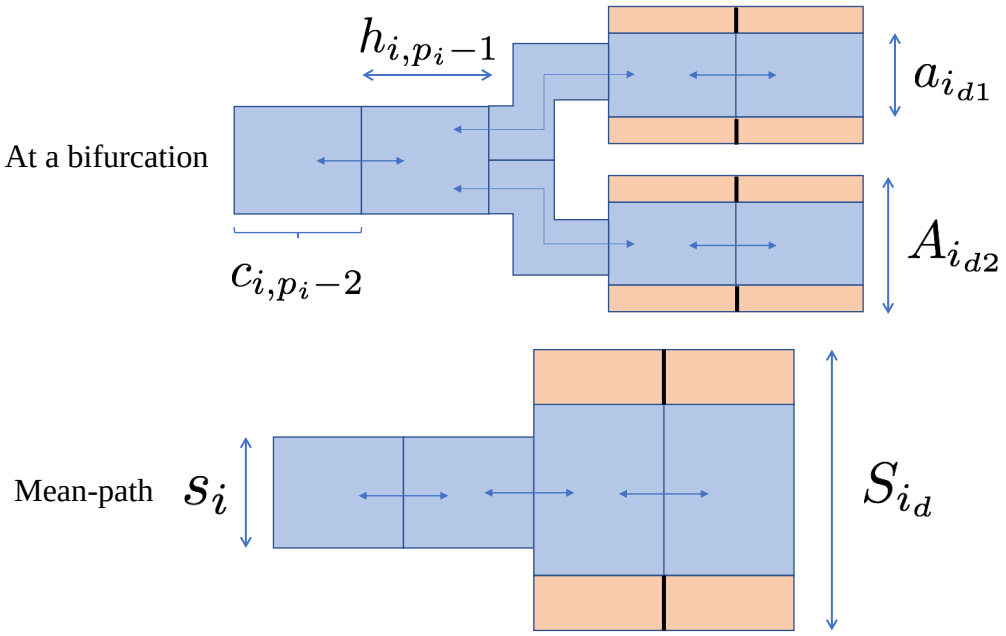

Figure SF4: Top: Sketch of a volumes and fluxes at a branching point between generations $j = N_z^{\text{cond}}$ and $N_z^{\text{cond}} + 1$. The cross-sectional areas of the daughter tubes with indices i_{d1} and i_{d2} are labelled, as well as the volume length and concentration. The z-shaped tubes are for visualisation purposes, highlighting the flux-splitting. Bottom: The equivalent volumes in a mean-path branch, no flux splitting takes place and both daughters are represented by the same tube with index i_d. The mean-path cross-sections are illustrated.

concentration field using the Crank-Nicholson discretisation of equation (16),

$$\begin{aligned} S_{i,x}^{n+1}c_{i,x}^{n+1} + \frac{\delta t}{2h_{i,x}}\left(F_{i,x+1/2}^{(a),n+1} + F_{i,x+1/2}^{(d),n+1} - F_{i,x-1/2}^{(a),n+1} - F_{i,x-1/2}^{(d),n+1}\right) = \\ S_{i,x}^{n}c_{i,x}^{n} - \frac{\delta t}{2h_{i,x}}\left(F_{i,x+1/2}^{(a),n} + F_{i,x+1/2}^{(d),n} - F_{i,x-1/2}^{(a),n} - F_{i,x-1/2}^{(d),n}\right) \end{aligned} \tag{40}$$

where the advective and diffusive fluxes are defined respectively as

$$F_{i,x+1/2}^{(a),n} = s_{i,x+1}\left[\max\left(u_{i,x+1}^{(l)}, 0\right)c_{i,x}^{n} + \min\left(u_{i,x+1}^{(l)}, 0\right)c_{i,x+1}^{n}\right] \tag{41}$$

$$F_{i,x+1/2}^{(d),n} = \begin{cases} \left(D_{i,x}^{(r)} + D_{i,x+1}^{(l)}\right)\left(\frac{c_{i,x+1}^{n} - c_{i,x}^{n}}{h_{i,x}+h_{i,x+1}}\right)\min\left(s_{i,x}\,,\, s_{i,x+1}\right) & \forall e_i \in \bar{\mathcal{E}}^{\text{cond}}, \\ 2D_0\left(\frac{c_{i,x+1}^{n} - c_{i,x}^{n}}{h_{i,x}+h_{i,x+1}}\right)\min\left(s_{i,x}^{(\text{eff})\text{n}}\,,\, s_{i,x+1}^{(\text{eff})\text{n}}\right) & \forall e_i \in \bar{\mathcal{E}}^{\text{acin}}, \end{cases} \tag{42}$$

such that the diffusive flux is determined by the smaller cross-section, and the advective flux is first-order upwinded. The area $s_{i,x}^{(\text{eff})}$ is the effective diffusive cross-section in the acinar ducts

$$s_{i,x}^{(\text{eff})\text{n}} = \phi S_{i,x}^{n} + (1-\phi)s_{i,x}. \tag{43}$$

At a terminal volume unit ($w_{i,p_i-1} \in e_i$ for any $e_i = e_{z,N_z^{\text{cond}}+N^{\text{acin}},k} \in \mathcal{L}$) the fluxes at the end of the

tree are set to zero $F^{(a)}_{i,p_i-1/2}, F^{(d)}_{i,p_i-1/2} = 0$. Finally, at a bifurcation

$$\begin{aligned} &S^{n+1}_{i,p_i-1}c^{n+1}_{i,p_i-1} + \frac{\delta t}{2h_{i,p_i-1}}\left(F^{(a),n+1}_{i_{d1},-1/2} + F^{(d),n+1}_{i_{d1},-1/2} + F^{(a),n+1}_{i_{d2},-1/2} + F^{(d),n+1}_{i_{d1},-1/2} - F^{(a),n+1}_{i,p_i-3/2} - F^{(d),n+1}_{i,p_i-3/2}\right) \\ &= S^{n}_{i,p_i-1}c^{n}_{i,p_i-1} - \frac{\delta t}{2h_{i,p_i-1}}\left(F^{(a),n}_{i_{d1},-1/2} + F^{(d),n}_{i_{d1},-1/2} + F^{(a),n}_{i_{d2},-1/2} + F^{(d),n}_{i_{d2},-1/2} - F^{(a),n}_{i,p_i-3/2} - F^{(d),n}_{i,p_i-3/2}\right). \end{aligned} \tag{44}$$

Fluxes at the bifurcation are defined consistently as

$$F^{(d),n}_{i_{d1},-1/2} = \left(D^{(r)}_{i,p_i-1} + D^{(l)}_{i_{d1},0}\right) s_{i_{d1},0}\left(\frac{c^n_{i_{d1},0} - c^n_{i,p_i-1}}{h_{i,p_i-1} + h_{i_{d1},0}}\right) \min\left(\frac{s_{j,k,z_T}}{s_{i_{d1},0} + s_{i_{d2},0}}, 1\right), \tag{45}$$

$$F^{(a),n}_{i_{d1},-1/2} = s_{i_{d1},0}\left[\max\left(u^{(l)}_{i_{d1},0}, 0\right) c^n_{i,p_i-1} + \min\left(u^{(l)}_{i_{d1},0}, 0\right) c^n_{i_{d1},0}\right], \tag{46}$$

$$F^{(d),n}_{i_{d2},-1/2} = \left(D^{(r)}_{i,p_i-1} + D^{(l)}_{i_{d2},0}\right) s_{i_{d2},0}\left(\frac{c^n_{i_{d2},0} - c^n_{i,p_i-1}}{h_{i,p_i-1} + h_{i_{d2},0}}\right) \min\left(\frac{s_{i,p_i-1}}{s_{i_{d1},0} + s_{i_{d2},0}}, 1\right), \tag{47}$$

$$F^{(a),n}_{i_{d2},-1/2} = s_{i_{d2},0}\left[\max\left(u^{(l)}_{i_{d2},0}, 0\right) c^n_{i,p_i-1} + \min\left(u^{(l)}_{i_{d2},0}, 0\right) c^n_{i_{d2},0}\right]. \tag{48}$$

The boundary condition for the concentration at the mouth is set using an extra node $c_{0,0,-1}$ such that $c_{0,0,-1} = 0$ if $u^{(l)}_{0,0,0} \geq 0$ and $c_{0,0,-1} = c_{0,0,0}$ if $u^{(l)}_{0,0,0} < 0$. The set of equations for $\mathbf{c}^{n+1}$ is a sparse linear system that we solve iteratively in C++ using the Eigen [9] 'BiCGSTAB' routine. To speed up computation we use the forward Euler method as an initial guess for the iterative computation

$$c^{n+1}_{i,x} \approx \frac{1}{S^{n+1}_{i,x}}\left[S^n_{i,x}c^n_{i,x} - \frac{\delta t}{h_{i,x}}\left(F^{(a),n}_{i,x+1/2} + F^{(d),n}_{i,x+1/2} - F^{(a),n}_{i,x-1/2} - F^{(d),n}_{i,x-1/2}\right)\right] \tag{49}$$

and at bifurcations

$$\begin{aligned} c^{n+1}_{i,p_i-1} \approx \frac{1}{S^{n+1}_{i,p_i-1}}\Bigg[S^n_{i,p_i-1}c^n_{i,p_i-1} - \frac{\delta t}{h_{i,p_i-1}}\Big(&F^{(a),n}_{i_{d1},-1/2} + F^{(d),n}_{i_{d1},-1/2} \\ &+F^{(a),n}_{i_{d2},-1/2} + F^{(d),n}_{i_{d2},-1/2} - F^{(a),n}_{i,p_i-3/2} - F^{(d),n}_{i,p_i-3/2}\Big)\Bigg] \end{aligned} \tag{50}$$

Following the update on the baseline model, we update the linearly perturbed equations on each linear perturbed tree. This involves computing the $O(\epsilon)$ changes to all equations, taking into account the difference in tree structure from the mean path model. These equations are then solved in the same manner as the mean path $O(\epsilon^0)$ equations, and depend on the updated $O(\epsilon^0)$ properties. To summarise, at each time step the simulation update is performed as follows

1. Update volumes through equation (35).
2. Update alveolar volumes through equation (7).
3. Update flow speed through incompressibility relations (38)-(39).
4. Update concentrations through equations (40) and (44).
5. Update linearly perturbed flows on each perturbed network (if included).
6. Update linearly perturbed concentration on each perturbed network (if included).

3 Multiple breath washout test and ventilation heterogeneity

The lung clearance index (LCI) is calculated by $\mathrm{LCI} = V_{\mathrm{exh}}(t_{\mathrm{LCI}})/V_{\mathrm{FRC}}^{\mathrm{approx}}(t_{\mathrm{LCI}})$ where $V_{\mathrm{exh}}(t)$ is the cumulative volume expired during washout. The FRC of the lung $V_{\mathrm{FRC}}^{\mathrm{approx}}(t)$ is itself approximated from the washout curve as

$$V_{\mathrm{FRC}}^{\mathrm{approx}}(t) = \frac{\int_0^t \dot{V}_{\mathrm{exh}}(\tilde{t}) c_m(\tilde{t}) \mathrm{d}\tilde{t}}{c_m(0) - c_m(t)} \tag{51}$$

where $c_m(t)$ is the concentration measured at the mouth, at $t = 0$ this is equal to the equilibrium concentration at end of wash-in, and at $t = t_{\mathrm{end}}$ is equal to the concentration recorded and the end of the final exhalation of the washout test.

The phase-III slopes $Sn_{\mathrm{III}}(N_{TO}(t_i))$ (units L^{-1}) of the individual exhalations are gradients of the final 'phase' (in tidal breathing) of the concentration-volume curve for a given exhalation n, normalised by the average concentration. Following [11] we use the final 50% of exhaled volume on each breath. Additionally, the index S_{cond} is the (fitted) slope of increase in Sn_{III} values versus $N_{TO}(t_i)$ between $N_{TO} = 1.5$-6.

In hyperpolarised inert gas MRI the fractional ventilation is computed as the inert gas dilution rate (correction for gas depolarisation) in each voxel of imaged lung tissue [12]. Here, we have similarly define fractional ventilation at the scale of the individual acini $\Omega_{z,\alpha}$ for breath number i as

$$FV_{z,\alpha}^{(i)} = \frac{\sum_{j,k} \int_0^{l_{z,j,k}} c_{z,j,k}(x, t_i) A_{z,j,k}(t_i) \mathrm{d}x}{\sum_{z,j,k} \int_0^{l_{z,j,k}} c_{z,j,k}(x, t_{i-1}) A_{z,j,k}(t_i - 1) \mathrm{d}x} \; \forall \left\{ j, k \mid e_{z,j,k} \in \mathcal{S}_{z,N_z^{\mathrm{cond}},\alpha} \right\}. \tag{52}$$

The mean fractional ventilation over the whole test is then simply $FV_{z,\alpha} = \sum_{i=0}^{N_{\mathrm{breaths}}} FV_{z,\alpha}^{i} / N_{\mathrm{breaths}}$ where N_{breaths} is the total number of breaths in the test.

3.1 Numerical modelling of multiple breath washout test

We have simulated a MBW test by applying a fixed flow rate at the mouth assumed to be sinusoidal $q_{\mathrm{mouth}} = \frac{2\pi V_T}{\tau} \sin\left(\frac{2\pi t}{\tau}\right)$ to approximate tidal breathing. This assumption puts a single constraint on the generic ventilation equation (6) (see section 2 for implementation).

The lung model is initialised with a constant (normalised) concentration $c = 1$ of the tracer gas everywhere. In order to accurately determine the LCI, a washout curve is constructed by measuring c_m at each exhalation as the final measured concentration and take the LCI value as the (interpolated) point on the N_{TO}-axis at which this curve crosses $0.025 c_m(t_{\mathrm{start}})$. Interpolation is used to obtain an LCI that is a continuous variable, sensitive to changes smaller than the turnover fraction V_T/V_{FRC}. In experimental tests variability in breath volumes and test repetition mean that LCI is not restricted to multiples of turnover fraction. Two simulated examples of washout measurements are shown in figure SF5.

The linear sensitivities of the MBW indices $\mathcal{I} \in \{\mathrm{LCI}, S_{\mathrm{cond}}\}$ to perturbations of the mean-path properties are acquired by retaining only linear terms. Following equation (25) the change in these parameters on the whole network $\mathcal{L}$ is approximated as

$$\Delta\mathcal{I} = \sum_{\mathcal{T}_z \in \mathcal{L}} \left\{ \sum_{e_{j,k} \in \mathcal{T}_z} \left[\delta\mathcal{I}^{(l,z,j)} \epsilon_{z,j,k}^{(l)} + \delta\mathcal{I}^{(a,z,j)} \epsilon_{z,j,k}^{(a)} \right] + \delta\mathcal{I}^{(K)} \sum_{\Omega_{z,\alpha} \in \Omega_z} \epsilon_{z,\alpha}^{(K)} \right\}. \tag{53}$$

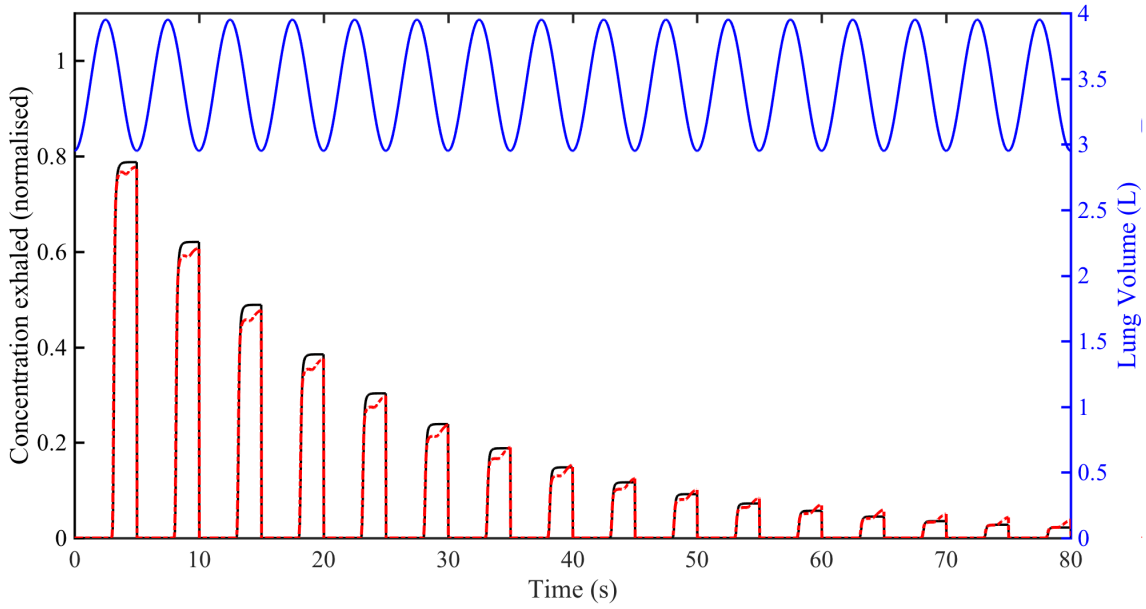

Figure SF5: Washout curves from mean-path model with no constrictions (black solid line) and radius constrictions of the central airways in RM lobe of 78% (red dashed line). The right axis corresponds to the lung volume (blue curve) (not including mouth dead-space) which is taken to be sinusoidal with a tidal volume of 1L.

The MBW indices $\mathcal{I}$ are measured at the mouth, so they have the same linear response $\delta\mathcal{I}^{(p,z,j)}$ to all perturbations of type p in a given generation j of network $\mathcal{T}_z$ where $z = \{\mathrm{RU}, \mathrm{RM}, \mathrm{RL}_{\mathrm{min}}, \mathrm{RL}_{\mathrm{maj}}, \mathrm{LU}, \mathrm{LL}_{\mathrm{min}}, \mathrm{LL}_{\mathrm{maj}}\}$.

The fractional ventilation $FV_{z,\alpha}$ depends on the relative position of perturbations on the network, but following equation (25) can still be reconstructed using the relevant combination of sensitivity functions. For acini $\Omega_{z,\alpha}$ in network $\mathcal{T}_z$ the linear change in FV is

$$\begin{aligned}\Delta FV_{z,\alpha} = &\sum_{\mathcal{T}_{\tilde{z}} \in \mathcal{L}\setminus\mathcal{T}_z} \left\{ \sum_{e_{j,k}\in\mathcal{T}_{\tilde{z}}} \left[\delta FV_z^{(l,\tilde{z},j)} \epsilon^{(l)}_{\tilde{z},j,k} + \delta FV_z^{(a,\tilde{z},j)} \epsilon^{(a)}_{\tilde{z},j,k} \right] + \delta FV_z^{(K,\tilde{z})} \sum_{\Omega_{\tilde{z},\tilde{\alpha}}\in\Omega_{\tilde{z}}} \epsilon^{(K)}_{\tilde{z},\tilde{\alpha}} \right\} \\ &+ \sum_{e_{j,k}\in\mathcal{T}_z} \left[\delta FV_z^{(l,j,j_{\mathrm{LCA}})} \epsilon^{(l)}_{z,j,k} + \delta FV_z^{(a,j,j_{\mathrm{LCA}})} \epsilon^{(a)}_{z,j,k} \right] + \delta FV_z^{(K,j,j_{\mathrm{LCA}})} \sum_{\Omega_{z,\alpha}\in\Omega_z} \epsilon^{(K)}_{z,\alpha}\end{aligned} \tag{54}$$

The linear sensitivities $\delta FV_z^{(p,\tilde{z},j)}$ for $p = \{l, a, K\}$ from trees $\mathcal{T}_{\tilde{z}} \neq \mathcal{T}_z$ depend only on perturbation generation and the tree perturbed, since all perturbations in the same generation of a different tree have the same effect. The second term counts the contributions $\delta FV_z^{(p,j,j_{\mathrm{LCA}})}$ from the within tree $\mathcal{T}_z$, which depend on the perturbation generation j and the LCA generation $j_{\mathrm{LCA}}(z, j, k, N_z^{\mathrm{cond}}, \alpha)$, as defined in equation (29).

4 Modelling random heterogeneity: summation of linear perturbations

In the linear perturbation limit, any model parameter is a linear superposition of the linear sensitivity functions weighted by the perturbations (see equation (25)). Hence, if the perturbations are defined as random variables from a multi-variate Gaussian, the variance in any model parameter $g_{z,j,k}$ can be

written as the sum of the covariance matrix weighted by the relevant linear sensitivities:

$$\begin{aligned}\mathrm{var}(g_{z,j,k}) = \sum_{\mathcal{T}_{z_1},\mathcal{T}_{z_2}\in\mathcal{L}} \Bigg\{ \sum_{e_{j_1,k_1}\in\mathcal{T}_{z_1}, e_{j_2,k_2}\in\mathcal{T}_{z_2}} \Bigg[\sum_{p_1,p_2\in\{a,l,K\}} \min(1-\delta_{p_1,K}+\delta_{j_1,N_{z_1}^{\mathrm{cond}}},1) \\ \min(1-\delta_{p_2,K}+\delta_{j_2,N_{z_2}^{\mathrm{cond}}},1)\mathrm{cov}\left(\epsilon^{(p_1)}_{z_1,j_1,k_1}, \epsilon^{(p_2)}_{z_2,j_2,k_2}\right) \delta g^{(p_1,z_1,j_1,k_1)}_{z,j,k} \delta g^{(p_2,z_2,j_2,k_2)}_{z,j,k} \Bigg] \Bigg\},\end{aligned} \tag{55}$$

where the functions $\min(1-\delta_{p_1,K}+\delta_{j_1,N_{z_1}^{\mathrm{cond}}},1)$ and $\min(1-\delta_{p_2,K}+\delta_{j_2,N_{z_2}^{\mathrm{cond}}},1)$ simply ensure that perturbations to the acinar elasticity occur only at the acinar generation $j = N^{\mathrm{cond}}$. We use this relation used to calculate the variance in MBW indices and FV values for following example cases.

4.1 Independent random heterogeneity

First, we have considered the case where perturbations are independent and normally distributed with zero mean and variance σ_p^2 such that $\epsilon^{(p)}_{z,j,k} = \mathcal{N}(0,\sigma_p^2)$. The covariance function is then $\mathrm{cov}(\epsilon^{(p)}_{z,j,k}, \epsilon^{(p')}_{j',k',z'}) = \delta_{j,j'}\delta_{k,k'}\delta_{z,z'}\delta_{p,p'}\sigma_p^2$ where $p \in \{a,l,K\}$ is the perturbation type (area, length or acinar elastance respectively). Using equations (55), and equation (26), the variance in an MBW index $\mathcal{I}$ is approximated as

$$\mathrm{var}(\mathcal{I}) = \sum_{\mathcal{T}_z\in\mathcal{L}} \left[2^{N_z^{\mathrm{cond}}} \left(\delta\mathcal{I}^{(K,z,N_z^{\mathrm{cond}})}\sigma_K\right)^2 + \sum_{p\in\{a,l\}} \sum_{j=0}^{N_z^{\mathrm{cond}}+N^{\mathrm{acin}}} 2^j \left(\delta\mathcal{I}^{(p,z,j)}\sigma_p\right)^2 \right]. \tag{56}$$

Unlike the MBW indices, the fractional ventilation values are associated with individual acini $\Omega_{z,\alpha}$. Therefore the linear sensitivities depend on the relative position of the defects. Again using equation (55) and equation (26), the variance in fractional ventilation (mean value over all breaths) is

$$\begin{aligned}\mathrm{var}(FV_{z,\alpha}) = &\sum_{\mathcal{T}_{z'}\in\mathcal{L}\setminus\mathcal{T}_z} \left[2^{N_{z'}^{\mathrm{cond}}} \left(\delta FV^{(K,z',N_{z'}^{\mathrm{cond}})}_{z,N_z^{\mathrm{cond}}}\sigma_K\right)^2 + \sum_{p\in\{a,l\}} \sum_{j=0}^{N_{z'}^{\mathrm{cond}}+N_{z'}^{\mathrm{acin}}} 2^j \left(\delta FV^{(p,z',j)}_{z,N_z^{\mathrm{cond}}}\sigma_p\right)^2 \right] \\ &+ \left(\delta FV^{(K,N_z^{\mathrm{cond}},N_z^{\mathrm{cond}})}_{z,N_z^{\mathrm{cond}}}\sigma_K\right)^2 + \sum_{j_{\mathrm{LCA}}=0}^{N_z^{\mathrm{cond}}-1} 2^{N_z^{\mathrm{cond}}-j_{\mathrm{LCA}}-1} \left(\delta FV^{(K,N_z^{\mathrm{cond}},j_{\mathrm{LCA}})}_{z,N_z^{\mathrm{cond}}}\sigma_K\right)^2 \\ &+ \sum_{p\in\{a,l\}} \Bigg[\sum_{j=1}^{N_z^{\mathrm{cond}}+N_z^{\mathrm{acin}}} \sum_{j_{\mathrm{LCA}}=0}^{\min(j,N_z^{\mathrm{cond}})-1} 2^{j-j_{\mathrm{LCA}}-1} \left(\delta FV^{(p,j,j_{\mathrm{LCA}})}_{z,N_z^{\mathrm{cond}}}\sigma_p\right)^2 \\ &\qquad + \sum_{j=0}^{N_z^{\mathrm{cond}}+N_z^{\mathrm{acin}}} 2^{j-\min(j,N_z^{\mathrm{cond}})} \left(\delta FV^{(p,j,\min(j,N_z^{\mathrm{cond}}))}_{z,N_z^{\mathrm{cond}}}\sigma_p\right)^2 \Bigg].\end{aligned} \tag{57}$$

The first line of equation (57) contains the contributions from perturbations in other mean-paths $z' \neq z$, which depend only on the mean-path and generation (for elasticity perturbations the generation is always $j = N_{z'}^{\mathrm{cond}}$. The second line contains elasticity perturbations in the same lobe, where the first term is the response to a perturbation in acinus Ω_α and the second term contains the response to all other elasticity perturbations. This term depends only on their LCA generation, where $j_{\mathrm{LCA}} \equiv j_{\mathrm{LCA}}(z,j,N_z^{\mathrm{cond}},k,\alpha)$ (defined in equation (13) of the main text) w.r.t. Ω_α. Similarly, the third line contains contributions from area and length perturbations that are not direct ancestors or descendents of $e_{N_z^{\mathrm{cond}},\alpha}$, while the final line accounts for area and length perturbations for those branches that are.

4.2 Correlated random heterogeneity

Second, we have considered airway sizes that are inherited from their parent branch such that geometry is correlated with the underlying structure of the lung. This inherited randomness is considered in [13] when modelling particle deposition in a stochastic lung model. In this case, we assume that the perturbations to length and area of branch $e_{j,k}$ are normally distributed with expected value given by the perturbations in their parent branch, such that

$$\begin{aligned} \boldsymbol{\epsilon}_{j,k,z} &= \mathcal{N}\left(\boldsymbol{\epsilon}_{j-1,\lfloor k/2 \rfloor,z}, \boldsymbol{\Sigma}\right), \\ \boldsymbol{\epsilon}_{j,k,z} &= \begin{pmatrix} \epsilon^{(a)}_{j,k,z} \\ \epsilon^{(l)}_{j,k,z} \end{pmatrix}, \ \boldsymbol{\Sigma} = \begin{pmatrix} \sigma_a^2 & \rho_{al}\sigma_a\sigma_l \\ \rho_{al}\sigma_a\sigma_l & \sigma_l^2 \end{pmatrix}. \end{aligned} \tag{58}$$

This results in a covariance between any two pairs of perturbations of $\mathrm{cov}(\boldsymbol{\epsilon}_{j,k,z}, \boldsymbol{\epsilon}_{j',k',z'}) = (j_{\mathrm{LCA}} + 1)\delta_{z,z'}\boldsymbol{\Sigma}$. The coefficient ρ_{al} quantifies the correlation between the area and length deviations of a given airway. To constrain the number of variables, we assume that the variance σ_p^2 and correlation coefficient ρ_{al} do not depend on generation. Using the redundancy relations (equations (10) and (11) in main text), and the expression for the covariance from above, the variance in the MBW indices $\mathcal{I}$ can be reduced to

$$\begin{aligned} \mathrm{var}(\mathcal{I}) = \sum_{\mathcal{T}_z \in \mathcal{L}} \Bigg\{ & 2^{N_z^{\mathrm{cond}}} \left(\delta\mathcal{I}^{(K,z,N_z^{\mathrm{cond}})}\sigma_K\right)^2 + \sum_{p_1,p_2 \in \{a,l\}} \sum_{j_1,j_2=0}^{N_z^{\mathrm{cond}}+N_z^{\mathrm{acin}}} 2^{j_1+j_2}\delta\mathcal{I}^{(p_1,z,j_1)}\delta\mathcal{I}^{(p_2,z,j_2)} \\ & \times \left[2^{-\min(j_1,j_2)}\left(\min(j_1,j_2)+1\right) + \sum_{j_{\mathrm{LCA}}=0}^{\min(j_1,j_2)-1} 2^{-(j_{\mathrm{LCA}}+1)}\left(j_{\mathrm{LCA}}+1\right) \right] \Sigma_{p_1,p_2} \Bigg\}. \end{aligned} \tag{59}$$

In the above, the elastance contribution (first term) remains the same, as this is assumed uncorrelated (both spatially and w.r.t. other variables). The second term sums all contributions from correlated perturbations to generations j_1 and j_2 of the same mean-path (perturbations are independent at inter-regional level). Of these, the first term in the square bracket counts those that are direct ancestors/descendents (*i.e.* $j_{LCA}(j_1,k_1,j_2,k_2) = \min(j_1,j_2)$) and the second counts all other possible relations (where $j_{LCA}(j_1,k_1,j_2,k_2) < \min(j_1,j_2)$).

Computing the variance of FV in a given mean-path $\mathrm{var}(FV_{z,\alpha})$ is more complex, as the contribution depends on the relative position of the two perturbations w.r.t. the mean path $\mathcal{T}_z$ and w.r.t. each other. This results in the sum

$$
\begin{aligned}
\mathrm{var}(FV_{z,\alpha}) = \sum_{\mathcal{T}_{z'}\in\mathcal{L}\setminus\mathcal{T}_z} \Bigg\{ & 2^{N_{z'}^{\mathrm{cond}}} \left(\delta FV_{z,N_z^{\mathrm{cond}}}^{(K,z',N_{z'}^{\mathrm{cond}})}\sigma_K\right)^2 + \sum_{p_1,p_2\in\{a,l\}} \Sigma_{p_1,p_2} \sum_{j_1,j_2=0}^{N_{z'}^{\mathrm{cond}}+N_{z'}^{\mathrm{acin}}} 2^{j_1+j_2}\delta FV_z^{(p_1,z',j_1)} \\
& \times\delta FV_z^{(p_2,z',j_2)} \left[2^{-\min(j_1,j_2)}\left(\min(j_1,j_2)+1\right) + \sum_{j'_{\mathrm{LCA}}=0}^{\min(j_1,j_2)-1} 2^{-(j'_{\mathrm{LCA}}+1)}\left(j'_{\mathrm{LCA}}+1\right)\right]\Bigg\} \\
& + \left(\delta FV_{z,N_z^{\mathrm{cond}}}^{(K,N_z^{\mathrm{cond}},N_z^{\mathrm{cond}})}\sigma_K\right)^2 + \sum_{j_{\mathrm{LCA}}=0}^{N_z^{\mathrm{cond}}-1} 2^{N_z^{\mathrm{cond}}-j_{\mathrm{LCA}}-1}\left(\delta FV_{z,N_z^{\mathrm{cond}}}^{(K,N_z^{\mathrm{cond}},j_{\mathrm{LCA}})}\sigma_K\right)^2 \\
& + \sum_{p_1,p_2\in\{a,l\}} \Sigma_{p_1,p_2} \sum_{j_1,j_2=0}^{N_z^{\mathrm{cond}}+N_z^{\mathrm{acin}}} 2^{j_1+j_2} \\
& \times \Bigg\{ 2^{-\min(j_1,N_z^{\mathrm{cond}})-\min(j_2,N_z^{\mathrm{cond}})}\delta FV_z^{(p_1,j_1,\min(j_1,N_z^{\mathrm{cond}}))}\delta FV_z^{(p_2,j_2,\min(j_2,N_z^{\mathrm{cond}}))} \\
& \quad \times \left[2^{-\max(\min(j_1-N_z^{\mathrm{cond}},j_2-N_z^{\mathrm{cond}}),0)}\left(\min(j_1,j_2)+1\right) + \sum_{j'_{\mathrm{LCA}}=N_z^{\mathrm{cond}}}^{\min(j_1,j_2)-1} 2^{-(j'_{\mathrm{LCA}}+1-N_z^{\mathrm{cond}})}\left(j'_{\mathrm{LCA}}+1\right)\right] \\
& \quad + 2^{-\min(j_1,N_z^{\mathrm{cond}})}\left[\sum_{j_{\mathrm{LCA}}^{(2)}=0}^{\min(j_2,N_z^{\mathrm{cond}})-1} 2^{-(j_{\mathrm{LCA}}^{(2)}+1)}\left(\min(j_1,j_{\mathrm{LCA}}^{(2)})+1\right)\delta FV_z^{(p_2,j_2,j_{\mathrm{LCA}}^{(2)})}\right] \\
& \quad + \sum_{j_{\mathrm{LCA}}^{(1)}=0}^{\min(j_1,N_z^{\mathrm{cond}})-1} 2^{-(j_{\mathrm{LCA}}^{(1)}+1)}\delta FV_z^{(p_1,j_1,j_{\mathrm{LCA}}^{(1)})} \\
& \quad \times \Bigg[2^{-\min(j_2,N_z^{\mathrm{cond}})}\delta FV_z^{(p_2,j_2,\min(j_2,N_z^{\mathrm{cond}}))}\left(\min(j_2,j_{\mathrm{LCA}}^{(1)})+1\right) + \sum_{j_{\mathrm{LCA}}^{(2)}=0}^{\min(j_2,N_z^{\mathrm{cond}})-1}\delta FV_z^{(p_2,j_2,j_{\mathrm{LCA}}^{(2)})} \\
& \qquad \times \Bigg(\left\{1-\delta_{j_{\mathrm{LCA}}^{(1)},j_{\mathrm{LCA}}^{(2)}}\right\} 2^{-(j_{\mathrm{LCA}}^{(2)}+1)}\left\{\min(j_{\mathrm{LCA}}^{(1)},j_{\mathrm{LCA}}^{(2)})+1\right\} \\
& \qquad\quad + \delta_{j_{\mathrm{LCA}}^{(1)},j_{\mathrm{LCA}}^{(2)}} \Bigg\{ 2^{-\min(j_1,j_2)}\left[\min(j_1,j_2)+1\right] \\
& \qquad\qquad + \sum_{j'_{\mathrm{LCA}}=j_{\mathrm{LCA}}^{(1)}+1}^{\min(j_1,j_2)-1} 2^{-(j'_{\mathrm{LCA}}+1)}\left(j'_{\mathrm{LCA}}+1\right)\Bigg\}\Bigg)\Bigg]\Bigg\}\Bigg\}.
\end{aligned}
\tag{60}
$$

The first two lines contains the contributions from other mean-paths ($\mathcal{T}_{z'} \neq \mathcal{T}_z$). Within that sum, the first term is the contribution from the (independent) elastance perturbations and the second sums contributions from pairs of airway perturbations (at generations j_1, j_2), where the first term in the square bracket counts the cases where j_1 and j_2 are direct ancestors/descendants of one another, and the second counts all of the other cases where they have mutual LCA generation $j'_{\mathrm{LCA}} < \min(j_1, j_2)$. The third line contains the terms for elastance perturbations within $\mathcal{T}_z$ with the first term contributing the case where the perturbation is to the acinus Ω_α and the second counts all perturbations to other

acini, grouped by their LCA generation j_{LCA} w.r.t Ω_α.

The remaining lines of equation (60) (fourth line onwards) contain all of the contributions from airway perturbations (at generations j_1, j_2) within $\mathcal{T}_z$. The fifth and sixth lines contain the contributions for when e_{j_1,k_1} and e_{j_2,k_2} are both direct ancestors or descendants of $e_{N_z^{\mathrm{cond}},\alpha}$, where the first term in the square bracket counts terms where e_{j_1,k_1} and e_{j_1,k_1} are direct ancestors/descendants of one another (always true if $j_1 \leq N_z^{\mathrm{cond}}$ or $j_2 \leq N_z^{\mathrm{cond}}$), while the second term counts the terms where they have LCA generation $j'_{\mathrm{LCA}} \geq N_z^{\mathrm{cond}}$ (possible only when $j_1 > N_z^{\mathrm{cond}}$ and $j_2 > N_z^{\mathrm{cond}}$). The seventh line counts the terms where e_{j_1,k_1} only is a direct ancestor or descendant of $e_{N_z^{\mathrm{cond}},\alpha}$. Finally, the eighth line onwards contains all the terms where e_{j_1,k_1} is not a direct ancestor or descendant of $e_{N_z^{\mathrm{cond}},\alpha}$ (it has LCA generation $j^{(1)}_{\mathrm{LCA}} < \min(j_1, N_z^{\mathrm{cond}})$ w.r.t. $e_{N_z^{\mathrm{cond}},\alpha}$). Within that the first term in the square bracket contains the contribution for terms where e_{j_2,k_2} is a direct ancestor or descendant of $e_{N_z^{\mathrm{cond}},\alpha}$. Otherwise, e_{j_2,k_2} has LCA generation $j^{(2)}_{\mathrm{LCA}} < \min(j_2, N_z^{\mathrm{cond}})$ w.r.t. $e_{N_z^{\mathrm{cond}},\alpha}$. In that case there are two further possibilities to consider, if $j^{(1)}_{\mathrm{LCA}} \neq j^{(2)}_{\mathrm{LCA}}$ then the two perturbations cannot be direct ancestors/descendants of one another and their LCA generation w.r.t. each other is $\min(j^{(1)}_{\mathrm{LCA}}, j^{(2)}_{\mathrm{LCA}})$ (tenth line), otherwise one has to count the different possible relations between e_{j_1,k_1} and e_{j_2,k_2} (eleventh and twelfth lines) as before.

4.3 Fractional ventilation distribution

The distribution of Fractional Ventilation in any mean-path is, in the linear limit, a normal distribution $P(FV_{z,\alpha})$ with mean $\bar{FV}_z$ and variance given by either (57) or (60). It follows that the overall probability density functions plotted in Fig 4 of the text, which represent the distribution of FV in the whole lung, are simply computed from a weighted sum of the relevant normal distributions

$$P(FV_\alpha) = \frac{\sum_{\mathcal{T}_z \in \mathcal{L}} 2^{N_z^{\mathrm{cond}}} P(FV_{z,\alpha})}{\sum_{\mathcal{T}_z \in \mathcal{L}} 2^{N_z^{\mathrm{cond}}}}. \tag{61}$$

References

[1] Horsfield K, Dart G, Olson DE, Filley GF, Cumming G. Models of the human bronchial tree. J Appl Physiol. 1971;31(2):207–217. doi:10.1152/jappl.1971.31.2.207

[2] Pedley TJ, Schroter RC, Sudlow MF. The prediction of pressure drop and variation of resistance within the human bronchial airways. Respir Physiol. 1970;9(3):387–405. doi:10.1016/0034-5687(70)90094-0.

[3] Dutrieue B, Vanholsbeeck F, Verbanck S, Paiva M. A human acinar structure for simulation of realistic alveolar plateau slopes. J Appl Physiol. 2000;89(5):1859–67. doi:10.1152/jappl.2000.89.5.1859

[4] Henry FS, Llapur CJ, Tsuda A, Tepper RS. Numerical Modelling and Analysis of Peripheral Airway Asymmetry and Ventilation in the Human Adult Lung. J Biomech Eng. 2012;134(6):061001. doi:10.1115/1.4006809.

[5] Tsuda A, Henry FS, Butler JP. Gas and aerosol mixing in the acinus. Respir Physiol Neurobiol. 2008;163(1-3):139–149. doi:10.1016/j.resp.2008.02.010.

[6] Weibel ER, Sapoval B, Filoche M. Design of peripheral airways for efficient gas exchange. Respir Physiol Neurobiol. 2005;148(1-2 SPEC. ISS.):3–21. doi:10.1016/j.resp.2005.03.005.

[7] Scherer PW, Shendalman LH, Greene NM, Bouhuys A. Measurement of axial diffusivities in a model of the bronchial airways. J Appl Physiol. 1975;38(4):719–23. doi:10.1152/jappl.1975.38.4.719

[8] Haefeli-Bleuer B, Weibel ER. Morphometry of the human pulmonary acinus. Anat. Rec. 1988;220(4):401–414. doi:10.1002/ar.1092200410.

[9] Guennebaud G, Jacob B, Others. Eigen; 2010. Available from: `http://eigen.tuxfamily.org`.

[10] Whitfield CA. PULMsim v1.1; 2018. doi:10.5281/zenodo.1251974.

[11] Robinson PD, Latzin P, Verbanck S, Hall GL, Horsley A, Gappa M, et al. Consensus statement for inert gas washout measurement using multiple- and single- breath tests. Eur Respir J. 2013;41(3):507–522. doi:10.1183/09031936.00069712.

[12] Horn FC, Deppe MH, Marshall H, Parra-Robles J, Wild JM. Quantification of regional fractional ventilation in human subjects by measurement of hyperpolarized 3He washout with 2D and 3D MRI. J Appl Physiol. 2014;116(2):129–139. doi:10.1152/japplphysiol.00378.2013.

[13] Koblinger L, Hofmann W. Aerosol deposition calculations with a stochastic lung model. Acta Phys Hungarica. 1986;59(1):31–34. doi:10.1007/BF03055180.